Journal of Thermal Analysis, Vol. 38 (1992) 961-971

THERMAL BEHAVIOUR AND MICROSTRUCTURAL CHARACTERIZATION OF LANTHANIDE SULPHIDES

R. M. Rojas, M. J. Torralvo** and L. C. Otero-Diaz***

*INSTITUTO DE CIENCIA DE MINERALES, CSIC, SERRANO 113, 28006 MADRID, SPAIN
**DEPARTAMENTO DE QUIMICA INORGÁNICA, FACULTAD DE QUIMICAS, UNIVERSIDAD COMPLUTENSE, 28040 MADRID, SPAIN

Thermal decomposition processes of rare earth sesquisulfides Ln_2S_3 (Ln = Lu, Y and Er) in O_2 flow up to 1590 K, have been studied. Decomposition takes place through incomplete oxidations and overlapping decomposition reactions. Two intermediate phases such as Ln_2O_2S and $Ln_2O_2SO_4$ are formed before the final more stable phase Ln_2O_3 (C-type) is obtained. Microstructural studies show the poor crystallinity of the intermediate products.

Keywords: lanthanide sulphides, microstructural characterization

Introduction

In spite of the general similarities in physical and chemical properties of the lanthanide elements, the crystal chemistry of their sulphides as well as their electric and magnetic properties are very complex, making this an area who has attracted the attention of many solid state scientists [1]. It is well established that several structural types occur, polymorphy is common and there is a great variation in composition for some nominal stoichiometries. Defect structures with short and long range order in the form of modulated structures also occur [2, 3].

On the other hand, many difficulties are encountered in the thermal analysis of these materials. Under oxidizing conditions, the formation of a final oxide residue occurs through a number of interdependent and overlapping reactions, highly dependent on the availability of oxygen to the reaction site and on the rate of removal of the products of partial reactions [4]. Although some thermal studies have been carried out on mineral chalcogenides, rare earth sulphides have been scarcely studied by these methods [5–7]. Some work has been done on thermal decomposition of lanthanide sulphides or sulphates [8]. In order to investigate the stability and reactivity of some of these sulphides, in this paper

John Wiley & Sons, Limited, Chichester
Akadémiai Kiadó, Budapest

we report the results obtained from both thermal and microstructural studies carried out on Ln_2S_3 (Ln = Lu, Y and Er) in O_2 flow up to 1590 K. Starting materials and the several products formed during thermal decomposition have been characterized by X-ray powder diffraction, electron diffraction and electron microscopy.

Experimental methods

Sample preparation

The binary sulphides Ln_2S_3 (Ln = Lu, Y and Er) have been prepared by induction-heating graphite crucibles containing the corresponding oxide Ln_2O_3 (99.99%) in a stream of Ar (95%) + H_2S (5%) at 1773 K for three hours and then cooled to room temperature by switching off the furnace. The products obtained are: δ–Y_2S_3 green colour; δ-Er_2S_3 pink colour, both with the–δ-Ho_2S_3 structure type, in good agreement with previous results [1, 9, 10]. On the other hand, σ–Lu_2S_3 is grey colour and presents the α–Al_2O_3 structure type [1].

Experimental techniques

Differential thermal analysis (DTA) and thermogravimetric (TG) curves were simultaneously recorded on a Stanton STA 781 instrument, at 10 deg·min^{-1} heating rate, in O_2 flow. About 10 mg sample were used for each run. Batches of each lanthanide sulphides were also heated at some particular temperatures and then cooled in O_2 flow. These products were used for X-ray and electron microscopy studies. X-ray powder diagrams were recorded on a Siemens D-500 diffractometer with CuK_α (λ = 1.5418 Å) at a scan speed of 1° 2θ min^{-1}. Electron diffraction patterns and micrographs were taken on a JEOL 2000 FX (200 kV) electron microscope, fitted with a double tilting ±45° goniometer. Samples were ground under *n*-butanol and dispersed on Cu grids coated with holey-carbon support films.

Results and discussion

Differential thermal analysis (DTA) and thermogravimetric (TG) curves recorded for Ln_2S_3 (Ln = Lu, Y and Er) in O_2 flow, are depicted in Figs 1a, b and c respectively. ε–Lu_2S_3 experiments between room temperature and 910 K a continuous and rather small weight gain (≈0.6%). Products identified at this temperature correspond to a mixture of the hexagonal Lu_2O_2S phase as minor component and the corundom type Lu_2S_3 starting material. Between 910 and

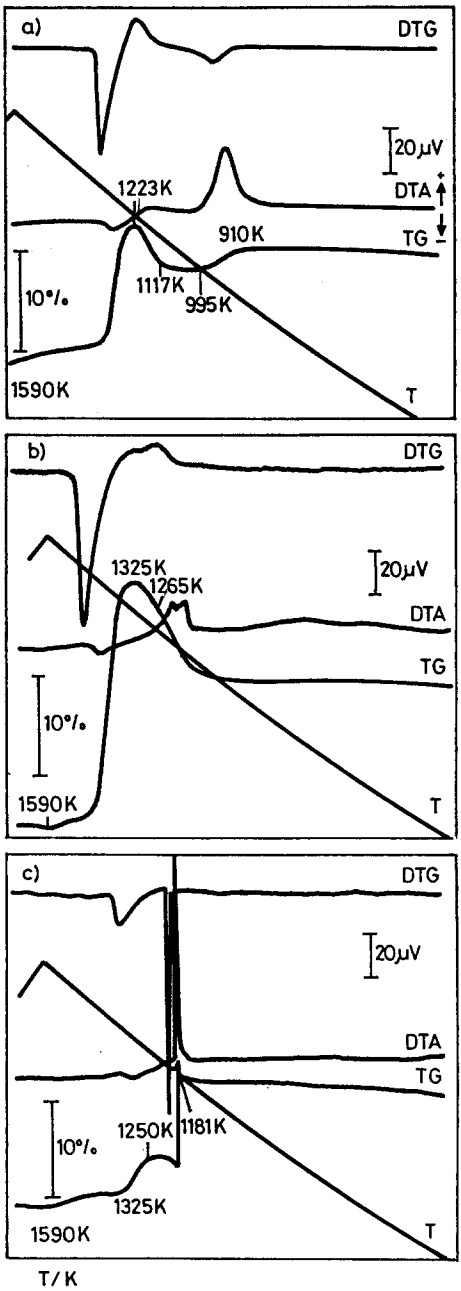

Fig. 1 Differential thermal analysis (DTA) and thermogravimetric (TG) curves for (a) Lu_2S_3, (b) Y_2S_3 and (c) Er_2S_3 samples, 10 deg·min^{-1} heating rate, O_2 flow (50 ml·min^{-1})

995 K, a weight loss of about 2% referred to the initial weight, takes place. Ot corresponds with the moderately exothermic effect observed in the DTA curve in the same temperature range. The experimental weight loss is considerably lower than calculated for the formation of Lu_2O_2S as the only component (7,17%). However, all diffraction maxima recorded on the residue formed at the latter temperature (995 K) can be assigned to the hexagonal Lu_2O_2S phase (Fig. 2a). Between 1117 and 1223 K the formation of the orthorhombic phase $Lu_2O_2SO_4$ takes place. X-ray pattern recorded at 1219 K can be fully indexed with cell parameters reported for this compound [11, 12], (Fig. 2b). However, neither the weight gain referred to the original sample (≈3%) nor the one referred to the intermediate Lu_2O_2S (≈5%) reasonably agree with the calculated according to the following reaction schemes: $Lu_2S_3 \rightarrow Lu_2O_2SO_4$ (7.17%) and $Lu_2O_2S \rightarrow Lu_2O_2SO_4$ (15.45%).

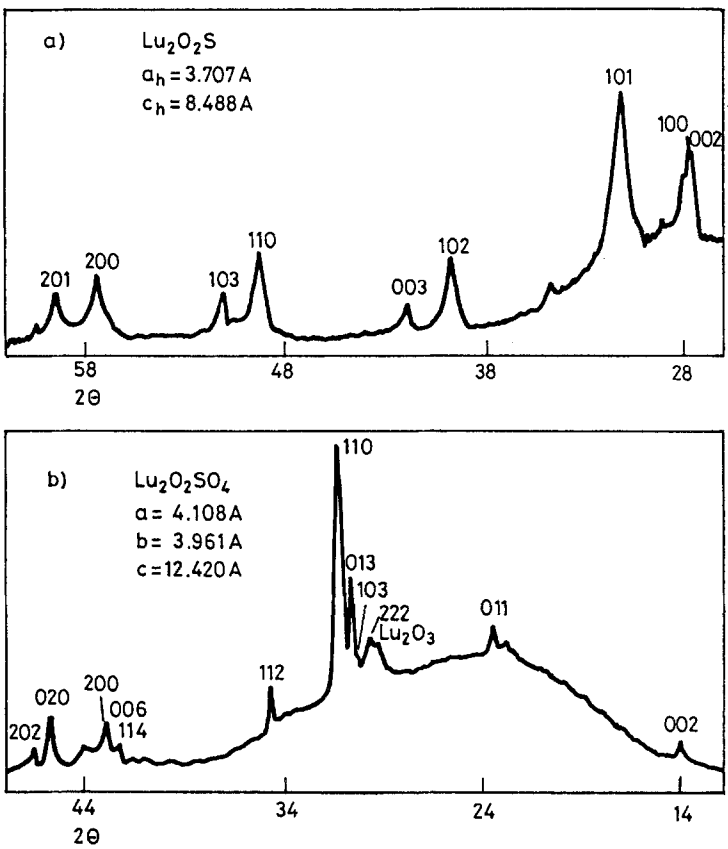

Fig. 2 X-ray powder diffraction patterns from Lu_2S_3 heated at (a) 995 K and (b) 1219 K (Lu_2O_3)

Electron microscopy and diffraction studies carried out on these samples reveals the following results. Figure 3a shows a Convergent Beam Electron Diffraction (CBED) pattern from one crystal of the sample heated up to 995 K. We may note the Zero Order Laue Zone (ZOLZ) and the FIRST Order Laue Zone (FOLZ) taken with the incident beam parallel to the [0001] zone axis of the hexagonal structure Lu_2O_2S. Figure 3b shows the corresponding low magnification image of the crystal, of about 600 nm length. Figure 3c shows a crystal marked by an arrow, of 500 nm width and 3600 nm length, with a mottled contrast. It comes from the product obtained at 1223 K. The corresponding diffraction pattern is given in Fig. 3d. Three types of reflections can be observed: the strong spots pattern, that can be indexed as the $[1\bar{1}0]$ of the orthorhombic $Lu_2O_2SO_4$ phase. The weak rings pattern corresponds to the Lu_2O_2S phase and finally, the very weak spots (like satellite reflections) with d-spacing of 7.4 Å, which corresponds to the {110} planes of the cubic Lu_2O_3 structure. These observations suggest that $Lu_2O_2SO_4$ is not formed as a pure single phase, and this result would account for the discrepancies observed between experimental and calculated weight variations. Cubic C–type Lu_2O_3 phase, a = 10.390 Å is obtained as a single final product at 1590 K, with an overall weight loss of 11.04%, in very good agreement with the theoretical one (10.76%) for the reaction $Lu_2S_3 \rightarrow Lu_2O_3$.

When heated in O_2 flow, monoclinic Yttrium sulphide δ–Y_2S_3 exhibits an apparently more unambiguous thermal behaviour. Orthorhombic $Y_2O_2SO_4$ is obtained at 1325 K, with an overall weight gain of 11.2%; the calculated for the reaction $Y_2S_3 \rightarrow Y_2O_2SO_4$ being 11.67%. Figure 4a shows an electron micrograph of the δ–Y_2S_3 sample heated up to 1325 K. It shows a polycrystal aggregate appearance, formed by small particles with an irregular contrast due to thickness effect. This is confirmed by the diffraction rings shown in Fig. 4b, which d-spacings correspond to $Y_2O_2SO_4$. However, the formation of $Y_2O_2SO_4$ is not a straightforward process. X-ray powder diagram recorded on Y_2S_3 heated up to 1265 K in an oxygen stream, clearly shows diffraction maxima of both hexagonal Y_2O_2S and orthorhombic $Y_2O_2SO_4$ phases (Fig. 5). Yttrium oxysulphate readily decomposes at 1337 K to the cubic C-type Y_2O_3 phase.

On the other hand, δ–Er_2S_3 on heated in O_2 flow behaves in a rather more unusual way. The sample experiments between room temperature and 1188 K a weight gain of about 2.8% and a mixture of hexagonal Er_2O_2S and the starting monoclinic δ–Er_2S_3 exits at this temperature, Fig. 6a. This result has been confirmed by TEM observations carried out on this residue. Figure 7a shows a low magnification image of a single crystal of Er_2O_2S and Fig. 7b is the corresponding electron diffraction pattern along the [0001] zone axis. Figure 7c shows a Selected Area Diffraction Pattern (SADP) of the monoclinic δ–Er_2S_3 along the

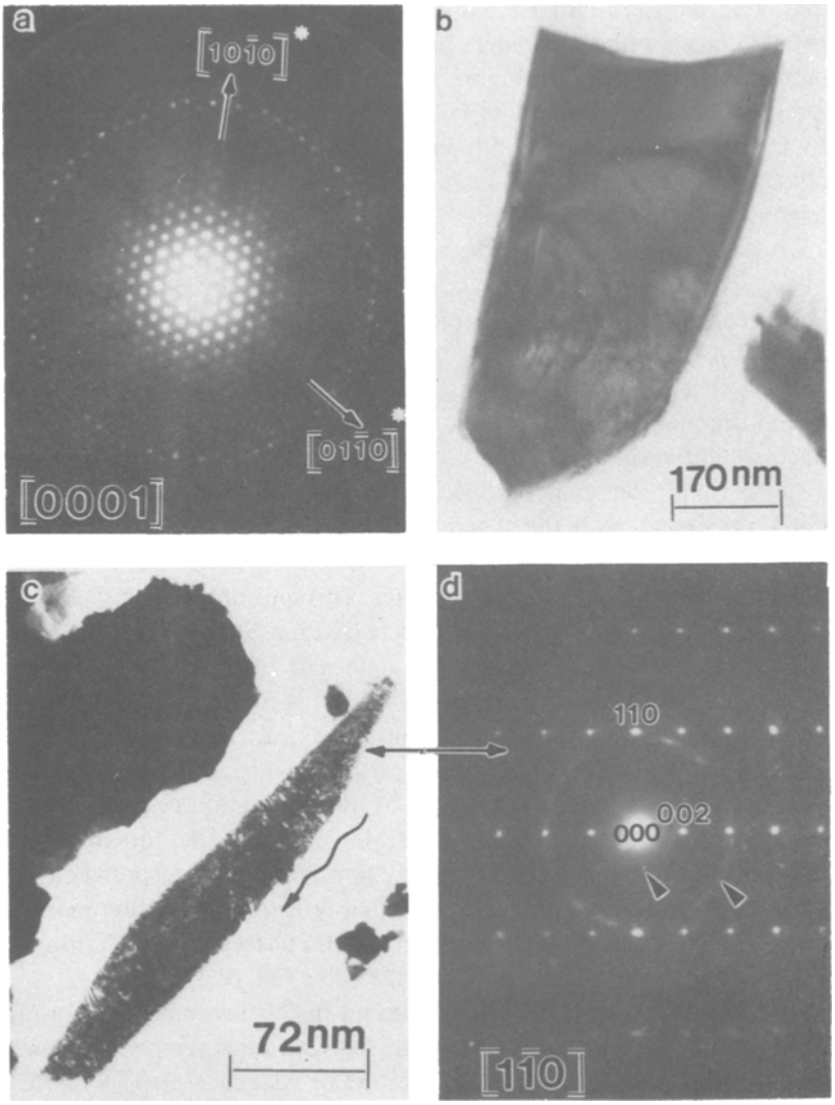

Fig. 3 (a) Microdiffraction pattern from the Lu_2O_2S phase along the [0001] zone axis. (b) corresponding low magnification image of the crystal. (c) Electron micrograph of a crystal showing a fish shape morphology from mainly the $Lu_2O_2SO_4$ phase. The spot pattern along the [1$\bar{1}$0] orientation is shown in (d). Extra spots and diffracted rings correspond to Lu_2O_3 and Lu_2O_2S respectively

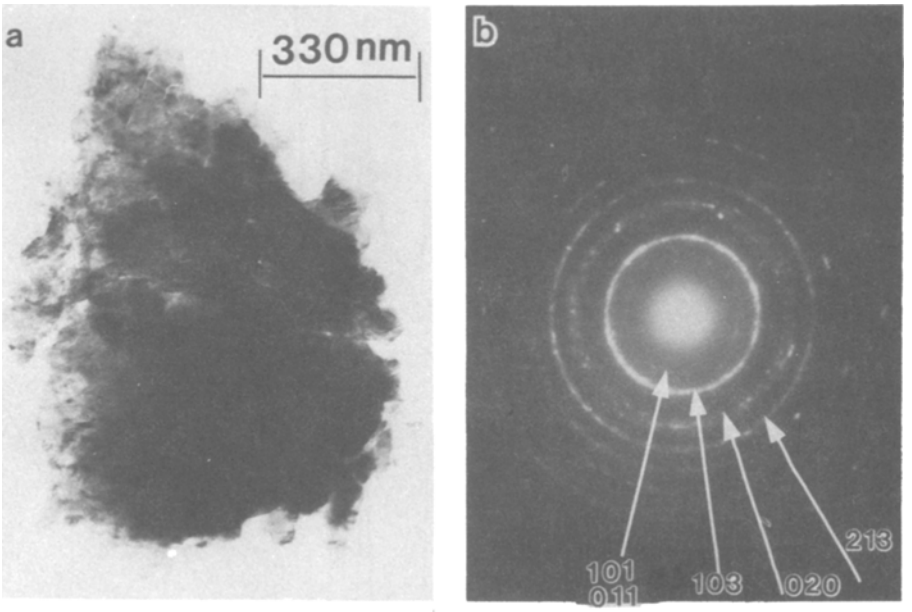

Fig. 4 (a) Low magnification image of a polycrystal from the phase $Y_2O_2SO_4$. (b) The corresponding diffracted rings pattern

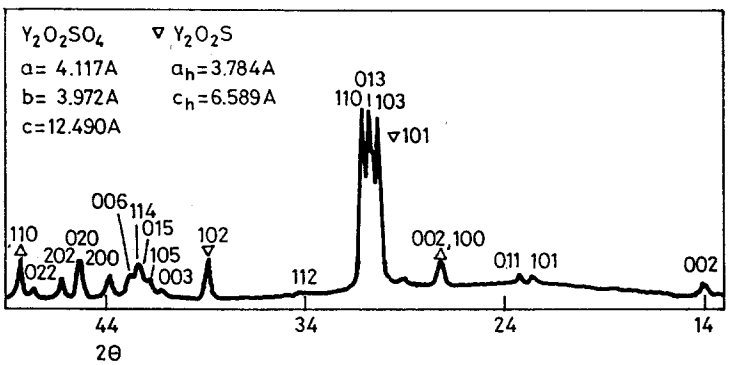

Fig. 5 X-ray powder diffraction pattern from Y_2S_3 heated at 1265 K

[021] zone axis. At the latter temperature, an extremely sharp exothermic peak appears in the DTA curve and the temperature of the sample rises up to 1223 K. This exothermic reaction corresponds to the abrupt weight loss recorded in the TG curve (9.64% referred to the sample weight at 1181 K, 7.08% referred to the initial sample). X-ray powder pattern recorded on the sample heated after this particular reaction clearly shows the cubic Er_2O_3 diffraction maxima. In addi-

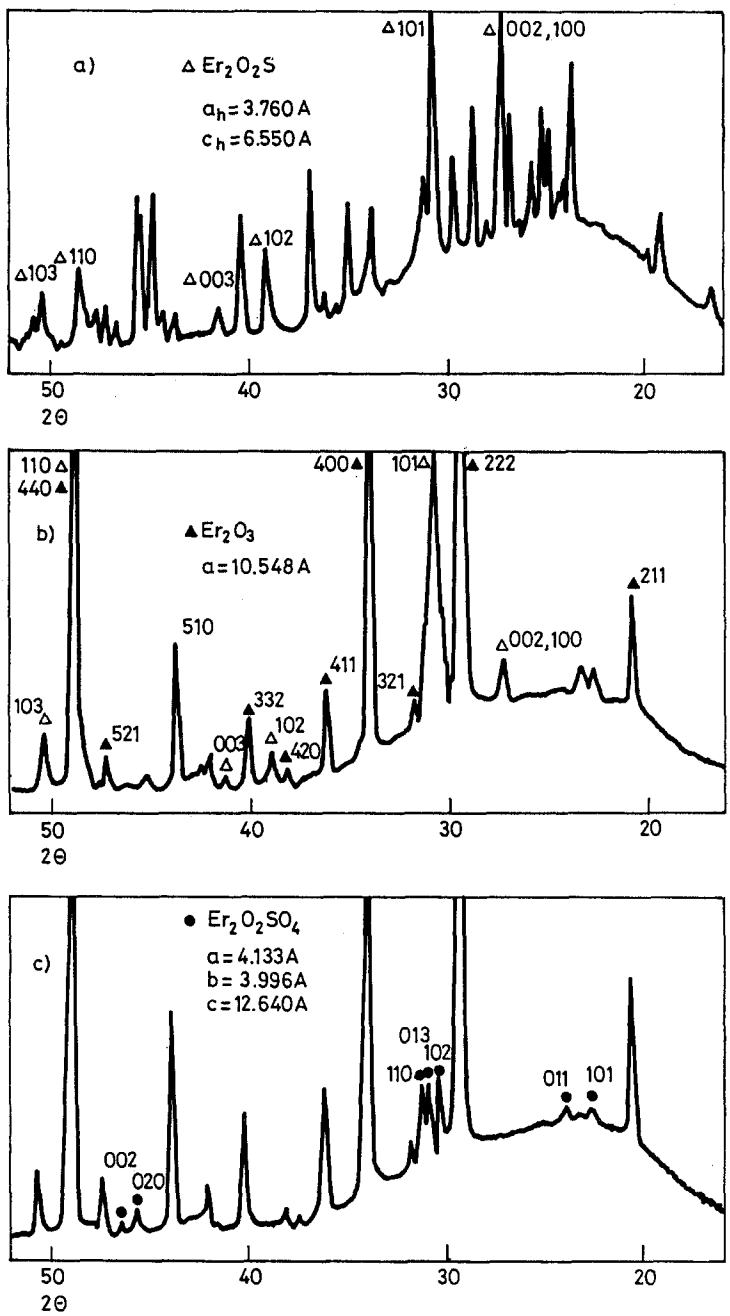

Fig. 6 X-ray powder diffraction pattern from Er_2S_3 heated at (a) 1173 K. Diffraction maxima without indexing correspond to monoclinic Er_2S_3), (b) 1188 K, (c) 1325 K (• $Er_2O_2SO_4$ non-indexed diffraction maxima correspond to the Er_2O_3 phase)

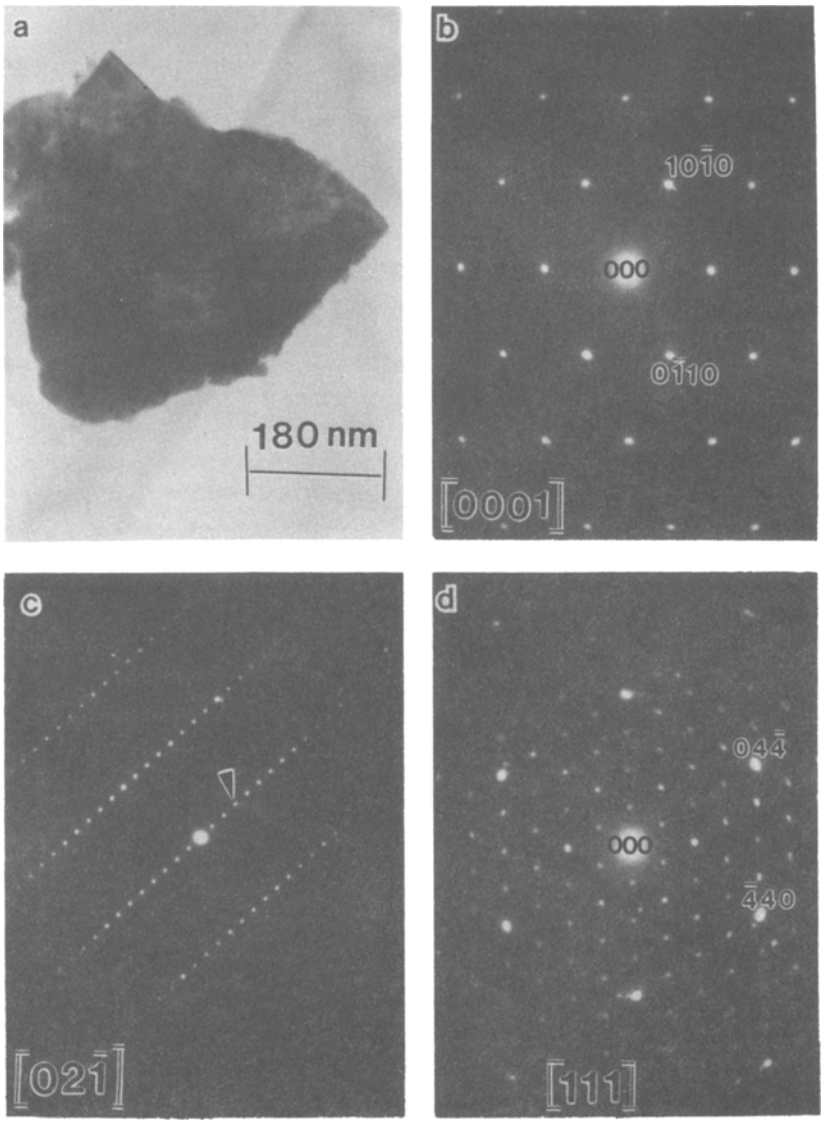

Fig. 7 (a) and (b) Electron micrograph and diffraction pattern from a single crystal of the Er_2O_2S phase. (c) and (d) Diffraction pattern from Er_2S_3 and Er_2O_3 respectively. Zone axis are indicated

tion, hexagonal Er_2O_2S phase diffraction maxima are also clearly observed. The broadening of diffraction maxima at 30–31.5 and 48–49° 2θ indicates the presence of some $Er_2O_2SO_4$ (Fig. 6b). The amount of the orthorhombic phase increases up to 1250 K, as does the weight of the sample. Finally, at 1325 K the C-type Er_2O_3 phase is the major component of the residue (Fig. 6c) and the oxide is obtained as an only phase at 1590 K, with an overall weight loss of 11%; calculated for the reaction $Er_2S_3 \rightarrow Er_2O_3$: 11.15%. In Fig. 7d, an electron diffraction pattern of the cubic Er_2O_3 (C-type) taken with the incident beam parallel to the [111] direction is shown.

Table 1 Phases identified during the thermal treatment of lanthanide sulphides

Sample	Temperature /K	Phases identified by X-ray powder diffraction
Lu_2S_3	910	$Lu_2S_3 + Lu_2O_2S$*
	995	Lu_2O_2S
	1219	$Lu_2O_2SO_4$
	1590	Lu_2O_3
Y_2O_3	1265	$Y_2O_2S + Y_2O_2SO_4$
	1325	$Y_2O_2SO_4 + Y_2O_2S$ *
	1590	Y_2O_3
Er_2S_3	1181	$Er_2S_3 + Er_2O_2S$
	1188	$Er_2O_3 + Er_2O_2S + Er_2O_2SO_4$*
	1250	$Er_2O_3 + Er_2O_2S + Er_2O_2SO_4$
	1325	$Er_2O_3 + Er_2O_2SO_4$
	1590	Er_2O_3

*minor component

From all the above indicated results, some conclusions can be pointed out. When Ln_2S_3 (Ln = Lu, Y and Er) compounds are heated in oxidizing atmosphere, the formation of Ln_2O_2S always takes place. Lu_2O_2S seems to be the more stable phase of the three Ln_2O_2S here identified. Ln_2O_3 is always obtained as the final product of thermal decomposition. Unlike the regular trends observed in thermal behaviour of lanthanide oxysulphides [8], rare earth sesquisulphides Ln_2S_3 (Ln = Lu, Y, and Er) show a very peculiar behaviour on heating, depending on lanthanide.

* * *

We wish to thank the Centro de Microscopia Electrónica, U.C.M.) for facilities. This research was supported by the CYCIT project MAT 89-0768.

References

1 J. Flahaut, Handbook on the Physics and Chemistry of Rare Earth, Eds. K. A. Gschneider and L. R. Eyring, North Holland Publishing Co., Amsterdam 1979, p. 1.
2 L. C. Otero-Diaz and B. G. Hyde, Acta Cryst., B29 (1983) 569.
3 L. C. Otero-Diaz, A. R. Landa-Cánovas and B. G. Hyde, J. Solid State Chem., 89 (1990) 237.
4 R. C. Mackenzie in 'Differential Thermal Analysis' 1, 7 (1970) 193.
5 L. C. Otero-Diaz, M. J. Torralvo and R. M. Rojas, React. Solids, 7 (1989) 143.
6 M. J. Torralvo, L. C. Otero-Diaz and R. M. Rojas, A. Quim., (in press).
7 H. W. Williams, Thermochim. Acta, 1 (1970) 253.
8 M. Leskelà and L. Niinistö, J. Thermal Anal., 18 (1980) 307; ibid, in W. Hemminger (Ed.) Thermal Analysis ICTA 80, 2 (1980) 247; ibid, in K. A. Gschneider and L. R. Eyring (Eds.), Handbook on the Physics and Chemistry of Rare Earth, 9 (1987) 91.
9 J. G. White, P. N. Jocom and S. Lemier, Inorg. Chem., 6 (1967) 1872.
10 B. G. Hyde and S. Anderson, Inorganic Crystal Structures, John Wiley & Sons, 1988.
11 R. Ballestracci and J. Mareschal, Mat. Res. Bull., 2 (1967) 993.
12 J. A. Fahey, Proc. 12th Rare Earth Res. Conf., (1976) 762.

Zusammenfassung — Im Sauerstoffstrom wurden bis zu einer Temperatur von 1590 K die thermischen Zersetzungsprozesse der Seltenerdensesquisulfide Ln_2S_3 (mit Ln = Lu, Y und Er) untersucht. Die Zersetzung läuft über unvollständige Oxidationsprozesse und überlappende Zersetzungsreaktionen ab. Vor der Bildung des Endproduktes Ln_2O_3 (C-Typ) werden die zwei weniger stabilen Intermediärphasen Ln_2O_2S und $Ln_2O_2SO_4$ gebildet. Eine Untersuchung der Mikrostruktur erwies die reine Kristallinität der intermediären Phasen.